JOURNAL OF APPLIED ELECTROCHEMISTRY 15 (1985) 485–493

*Interfacial electrical properties of electrogenerated bubbles**

N. P. BRANDON‡, G. H. KELSALL

Department of Mineral Resources Engineering, Imperial College, London SW7 2BP, UK

S. LEVINE, A. L. SMITH

Unilever Research, Port Sunlight Laboratory, Wirral, Merseyside L63 3JW, UK

Received 14 November 1982

Electrophoresis measurements on bubbles of electrogenerated hydrogen, oxygen and chlorine rising in a lateral electric field, are reported. In surfactant-free solutions, all bubbles displayed a point of zero charge of pH 2–3, i.e. they were negatively charged at pH > 3 and positively charged at pH < 2. The bubble diameter and electric field strength dependence of the electrophoretic mobilities, coupled with bubble rise rate measurements, indicated that the gas–aqueous solution interface was mobile, such that classical electrophoresis theory for solid particles could not be applied. Adsorption of anionic or cationic surfactants, in addition to modifying the apparent bubble charge, also tended to rigidify the bubble surface, so that at monolayer coverage the bubbles behaved as solid particles.

Nomenclature

c	electrolyte concentration (mol m^{-3})
d	bubble diameter (m)
E	electric field (V m^{-1})
g	gravitational constant (9.807 m s^{-2})
n_0	ionic number density (m^{-3})
q	charge density [(μ, m) C m^{-2}]
Q	charge [(μ, m) C]
r	bubble radius (m)
R	universal gas constant (8.314 J mol^{-1} K^{-1})
T	absolute temperature (K)
u	electrophoretic mobility (m^2 s^{-1} V^{-1})
v	electrophoretic velocity (m s^{-1})
ϵ	electrolyte permittivity (F m^{-1})
η	electrolyte viscosity (N m^{-2} s)
Γ	surface concentration (mol m^{-2})
k	Debye–Huckel parameter (m^{-1})
ρ	electrolyte density (kg m^{-3})
ρ'	gas density (kg m^{-3})
ζ	zeta potential (V)

1. Introduction

The effective charge density and electrical potential resulting from charge separation of gas–liquid interfaces is of importance in fine particle flotation, thin solution film formation, bubble coalescence and the evolution of gas at electrodes, the technological consequences of which are wide ranging.

When the solution contains ionic surfactants, the origin of any charge at the gas–liquid interface is not in doubt. However, in the (apparent) absence of such species, the mechanisms of charge separation are less clear, but presumably involve the adsorption/negative adsorption of electrolyte ions, especially H^+/OH^-. A simple electrolyte which increases the surface tension of the air–water interface must be negatively adsorbed. Unequal negative adsorption of oppositely charged ions such as H^+/OH^- will lead to charge separation and the development of an electric double layer.

Various authors [1–8] have centrifuged

*Paper presented at the International Meeting on Electrolytic Bubbles organized by the Electrochemical Technology Group of the Society of Chemical Industry, and held at Imperial College, London, 13–14 September 1984.

‡Present address: BP Research Centre, Chertsey Road, Sunbury-on-Thames, Middlesex TW16 7LN, UK.

0021-891X/85 $03.00 + .12

bubbles to the axes of rotating horizontal cylinders containing suitable electrolytes, and measured the bubble migration velocity in an applied field, taking this electrophoretic mobility as a measure of the interfacial charge. Others [9–11] have measured the Dorn potential of rising bubble swarms, and two groups [12–14] have electrogenerated oxygen bubbles at wire electrodes, measuring the electrophoretic mobilities of the rising bubbles in a horizontal electric field. All authors have observed substantial electrophoretic mobilities, corresponding to a negative charge at neutral pH, though the absence of adventitious anionic surfactant has not always been convincing.

The work reported here attempted to infer the nature of the charge separation at gas–solution interfaces from measurements of electrophoretic mobilities as a function of pH in simple surfactant-free electrolytes, to which cationic and anionic surfactants were added in subsequent experiments.

2. Experimental details

2.1. *Electrolyte preparation*

Surfactant-free water, a prerequisite for this work, was prepared by distillation, before being passed through columns of anionic (Duolite A101D) and mixed anionic/cationic (Zerolit DMF) exchange resins, then through activated charcoal, followed by redistillation from alkaline potassium permanganate and acidified potassium dichromate solutions to remove residual organic acids and bases, respectively. The whole system was kept under purified nitrogen including the receiver, from which water was drained into two mixing vessels, to which 'Aristar' grade (BDH plc) reagents were added. A high ionic strength electrolyte was prepared for the bubble growth cell (Fig. 1) and a more dilute solution (< 1 mol m^{-3}) for the electrophoresis cell (Fig. 2).

As even this grade of commercial electrolyte may contain surfactants, sodium sulphate, which was used for much of the work, was heated to red heat to decompose organic impurities and sealed into a glass ampule, which subsequently was broken inside the apparatus. Finally, all electrolytes were purged with swarms of electrogenerated bubbles from a pair of auxilliary Pt electrodes in each cell, and any residual surfactants, which would have been concentrated at the gas–electrolyte interface, were swept over a wier [15]. Some anodic oxidation of the surfactants may also have been responsible for the decrease in contamination levels with time.

2.2. *Cyclic voltametry*

Standard electrochemical instrumentation specified elsewhere [16, 17] was used to obtain cyclic voltamograms of a platinum microelectrode, as a semi-quantitative means of assessing the level of contamination by adsorbed surfactants [18]. Calibration voltamograms were obtained in surfactant-free electrolytes, to which known concen-

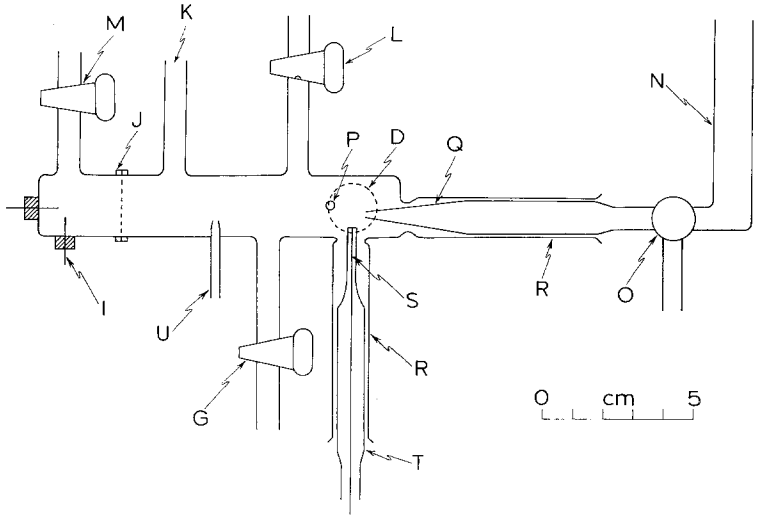

Fig. 1. Electrochemical cell for bubble growth at microelectrodes. (Labelling as for Fig. 2.)

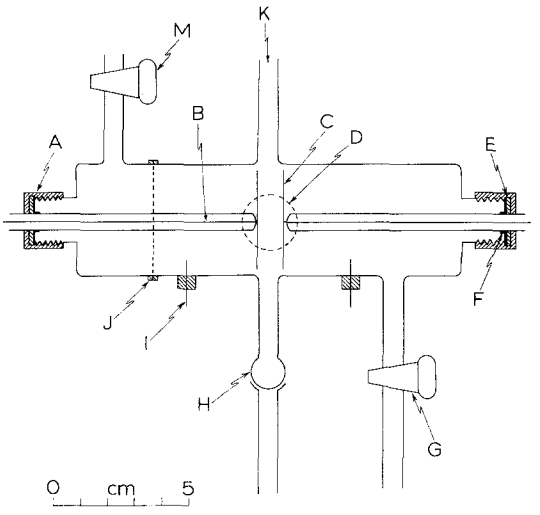

Fig. 2. Electrophoresis cell: A, screw cap for electrode adjustment; B, Pt wire sealed into glass; C, 30 × 20 mm Pt/Pd,H_2 or Ag/AgCl electrodes; D, Optical flat; E, Rubber seal; F, PTFE seal; G, 3 mm bore PTFE tap to drain; H, Ball and socket joint; I, Pt foil purging electrodes; J, Glass flange; K, Electrolyte inlet; L, Tap with drilled recess; M, 3 mm bore PTFE tap to vent; N, Reference electrode; O, 3 mm bore glass T tap; P, Counter electrode; Q, Luggin probe; R, 2 ml syringe barrel; S, Working electrode sealed in glass; T, Syringe plunger; U, Hydrogen (or oxygen) inlet.

trations of sodium dodecyl sulphate (SDoS) or sodium dodecyltrimethylammonium bromide (DoTAB) were subsequently added. By comparison of these data with those obtained in electrolytes thought to contain adventitious surfactants, an estimate of the level of contamination could be made.

2.3. *Bubble rise rates*

The rise rate of bubbles in electrolytes was found to be sensitive to the level of surfactant contamination, surfactant adsorption at the gas–solution interface inducing surface tension gradients, rigidifying the bubble surface, and so lowering the rise rate.

Single bubbles were produced electrolytically and transferred via a modified tap to the rise rate apparatus, consisting of a 40 mm diameter glass column to which two silicon photodiodes were clamped 0.1 m apart. The rise rate was measured by detecting the bubble's interruption of the light from a fibre optic source on a digital storage oscilloscope. The bubble diameter was measured at the top of the column using a calibrated microscope. Two Pt electrodes were sealed into the base of the column to enable the effect of bubble cleaning of the electrolyte to be studied.

2.4. *Electrophoresis*

The lower cell, shown in Fig. 1, was used to determine the growth kinetics and departure diameters of bubbles generated at vertically mounted microelectrodes, details of which are given elsewhere [16, 17]. Bubbles were transferred into the upper cell (Fig. 2) using a glass tap into which a small recess had been drilled.

Two Roband Varex 60-5 power supplies connected in series were used to apply up to 120 V between two electrodes, palladium-plated Pt (hydrogen) in millimolar sodium sulphate electrolytes and Ag/AgCl in millimolar potassium chloride media, reversible electrodes being used to prevent gas evolution. To enable the applied field to be maintained across the electrolyte with minimal current flow (< 2 mA), the pH range was restricted to 2–12. Bubble deflection was studied using a microscope, TV camera, video recorder and monitor.

Latterly, high purity dodecyltrimethylammonium bromide (DoTAB, Kodak plc) and sodium dodecylsulphate (SDoS, BDH plc) surfactants, the gas–liquid adsorption isotherms for which were known [19], were added to the above electrolytes. All experiments were carried out at 295 ± 2 K and a pressure of 101 ± 2 kN m^{-2}.

3. Results and discussion

3.1. *Cyclic voltametry*

The effect of SDoS additions on cyclic voltamograms of a Pt electrode in 0.1 kmol H_2SO_4 m^{-3}, are shown in Fig. 3. At low potentials the hydrogen adsorption desorption peak currents decreased with increasing surfactant concentration, and at higher potentials the oxidation of platinum occurred at more anodic potentials, though with the passage of more charge in its formation and reduction. This is in approximate agreement with the results of Conway *et al.* [18], whose surfactants were adventitious and so of unspecified nature and concentration.

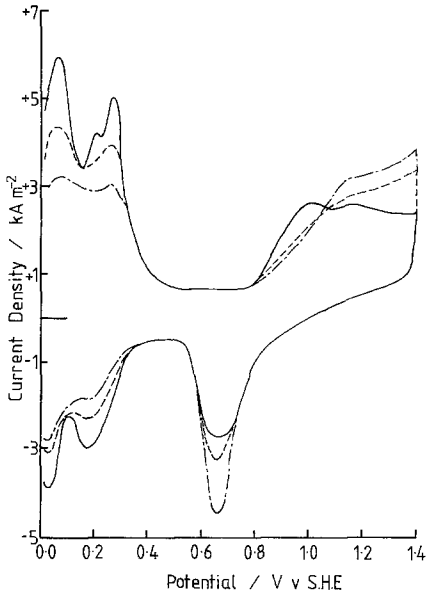

Fig. 3. Effect of SDoS surfactant concentration on Pt cyclic voltamograms at 0.1 V s^{-1} in 0.1 kmol H_2SO_4 m^{-3}. —— surfactant-free, — — — 10^{-3} mol SDoS m^{-3}, —·—·— 1 mol SDoS m^{-3}.

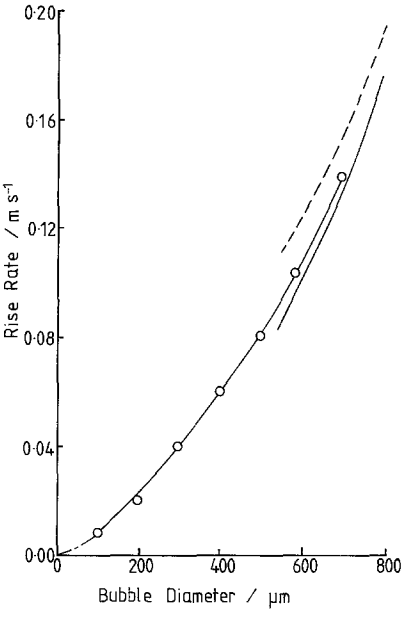

Fig. 4. Bubble rise rate in purified water compared with that predicated in surfactant-free water. —·— $Re < 1$, —— $50 < Re < 800$, Levich [20], — — — Moore [21], ○ experimental results.

3.2. *Bubble rise rate*

The rise rate of bubbles was found to be particularly sensitive for detection of surfactant contamination in electrolytes. Fig. 4 shows a comparison of bubble rise rate in 'as distilled' water with that predicted theoretically for surfactant-free water, for which Levich [20] gives:

$$v = \frac{1}{3\eta} r^2 g(\rho - \rho') \text{ for } Re < 1 \qquad (1)$$

$$v = \frac{1}{9\eta} r^2 g(\rho - \rho') \text{ for } 50 < Re < 800 \qquad (2)$$

where ρ is the density of the liquid of viscosity η, and ρ' is the density of the gas bubble of radius r. While the experimental data gave good agreement (Fig. 4) with these theoretical equations, a better fit (i.e. the experimental data lay just *below* the theoretical curve) for $Re > 50$ was obtained with Moore's curve [21], obtained by expansion of the Levich model to allow for boundary layer perturbation.

However, addition of electrolyte introduced surfactant contamination, as indicated by the decrease in bubble rise rate (Fig. 5 and 6), allowing for the small increase in electrolyte viscosity. By purging the electrolyte with a swarm of bubbles electrogenerated at auxilliary electrodes in each cell, the electrolyte purity improved with time, attaining the quality of 'as purified' water after about 3 h (Fig. 7). The same purity enhancement was achieved by prior heating of solid electrolytes (Na_2SO_4 or KCl).

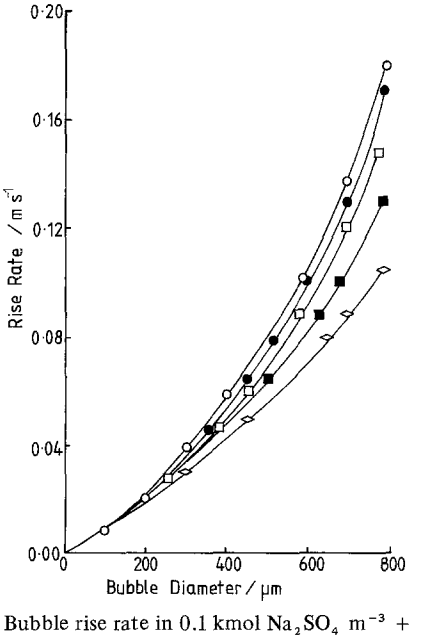

Fig. 5. Bubble rise rate in 0.1 kmol Na_2SO_4 m^{-3} + sulphuric acid. ○ surfactant-free, • 0.001, □ 0.01, ■ 0.1, ◇ 1 kmol H_2SO_4 m^{-3}.

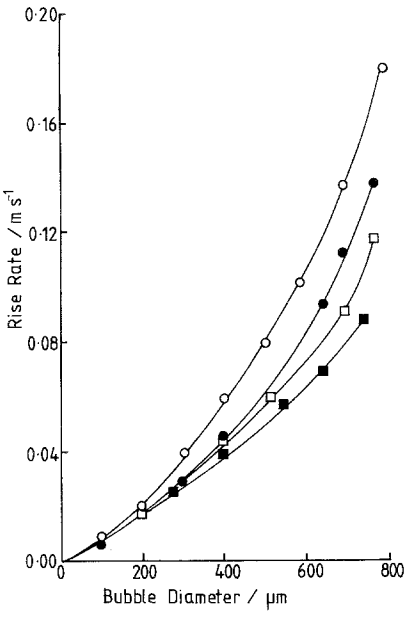

Fig. 6. Bubble rise rate in 0.1 kmol Na_2SO_4 m^{-3}, ○ surfactant-free, plus ● 0.01, □ 0.1, ■ 1 kmol NaOH m^{-3}.

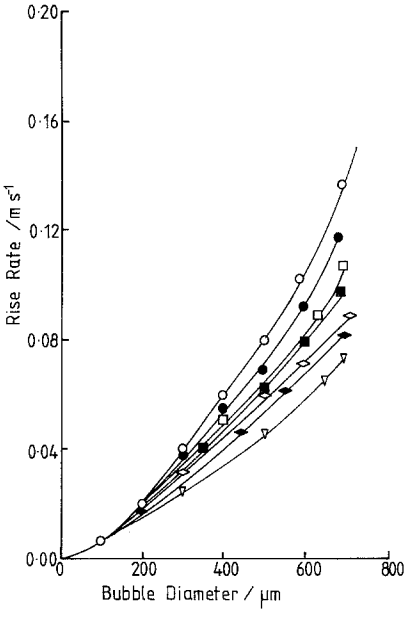

Fig. 8. Effect of DoTAB surfactant on bubble rise rate. ▽ 1, ◆ 10^{-1}, ◇ 10^{-2}, ■ 10^{-3}, □ 10^{-4}, ● 10^{-5} mol DoTAB m^{-3}, ○ surfactant-free 0.01 kmol Na_2SO_4 m^{-3}.

Fig. 8 illustrates the sensitivity of bubble rise rate to very low concentrations of surfactant ($> 10^{-5}$ mol m^{-3}). Comparison of this with the data in Figs. 6 and 7, showed that molar sodium hydroxide and sulphuric acid introduced the equivalent of 10^{-1} and 10^{-2} mol m^{-3} of surfactant contamination, respectively. However, following bubble cleaning the levels of surfactant impurities decreased to the equivalent of $< 10^{-5}$ mol DoTAB m^{-3}.

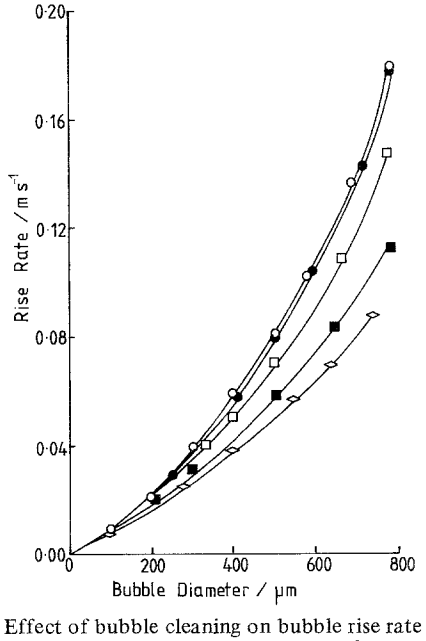

Fig. 7. Effect of bubble cleaning on bubble rise rate in 0.01 kmol Na_2SO_4 m^{-3} + 1 kmol NaOH m^{-3}, ● 3, □ 2, ■ 1, ◇ 0 h purge, ○ purified water.

3.3. *Bubble electrophoretic mobility measurements*

3.3.1. Surfactant-free electrolytes. Figs. 9–11 show the influence of pH on the electrophoretic mobilities of electrogenerated hydrogen, oxygen and chlorine bubbles, respectively. All the gases displayed a point of zero charge at pH 2–3, in approximate agreement with the value of pH 1–2 proposed previously [7] for nitrogen bubbles, indicating an independence of the type or source of the gas. That the negative bubble charge displayed at pH > 3 could be reversed rather than merely reduced to zero at pH < 2, removed any remaining doubts that the bubble charge was due to surfactant contamination. However, the reasons for preferential adsorption of OH^- at the gas–solution interface are not immediately apparent.

Fig. 12 shows that the electrophoretic mobility was linearly dependent on bubble diameter over the pH range 4–10, which is not predicted by

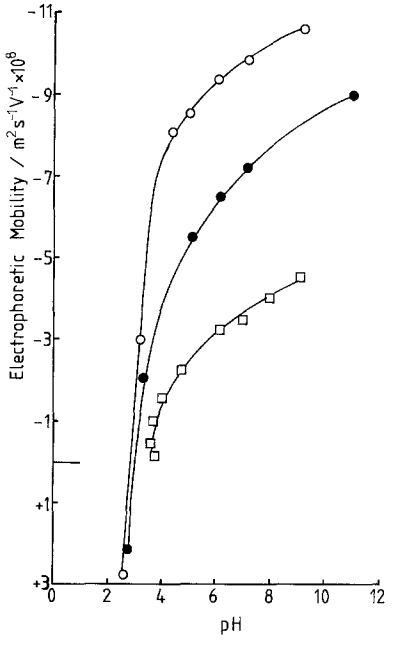

Fig. 9. Effect of pH on the electrophoretic mobility of hydrogen bubbles in 1 mol Na_2SO_4 m^{-3}, ○ 200 μm, ● 120 μm, □ 30 μm diameter.

classical theory for the electrophoresis of solid particles [22]. This reflected the mobile nature of the gas–liquid interface, which produced charge separation around the bubble through either:

i. hydrodynamic flow induced by a vertically rising bubble,

ii. polarization of surface charge by the horizontal electric field.

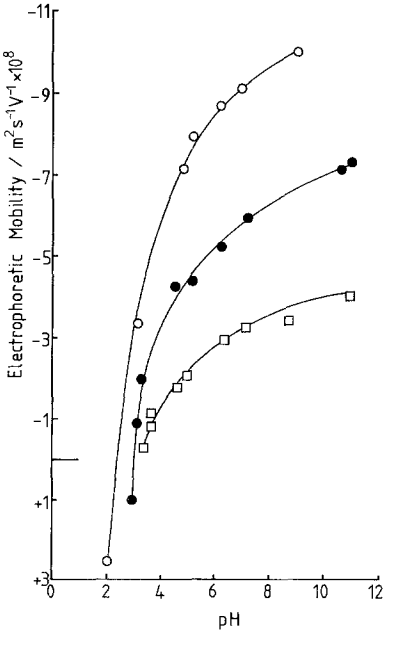

Fig. 10. Effect of pH on the electrophoretic mobility of oxygen bubbles in 1 mol Na_2SO_4 m^{-3}, ○ 180 μm, ● 100 μm, □ 30 μm diameter.

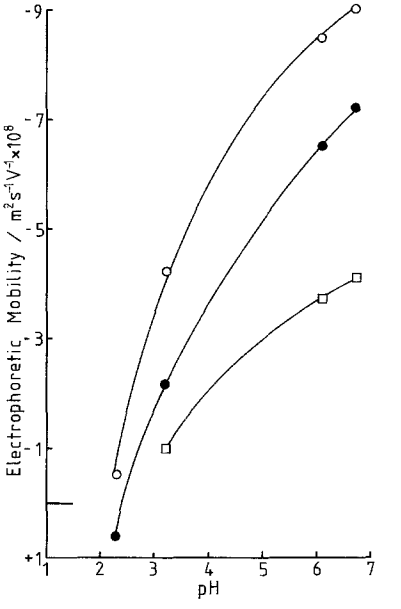

Fig. 11. Effect of pH on the electrophoretic mobility of chlorine bubbles in 1 mol KCl m^{-3}, ○ 150 μm, ● 100 μm, □ 30 μm diameter.

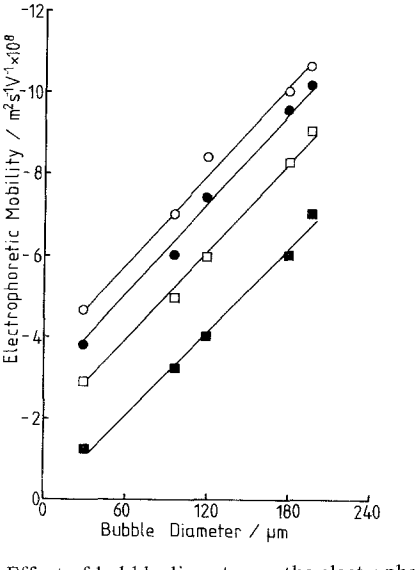

Fig. 12. Effect of bubble diameter on the electrophoretic mobility of oxygen and hydrogen bubbles in 1 mol Na_2SO_4 m^{-3} at pH 4 (■), 6 (□), 8 (●) and 10 (○).

A linear dependence of electrophoretic mobility on diameter has been predicted for charged mercury drops, which also exhibit a mobile interface. A theoretical treatment of bubble electrophoresis, adapted from that for mercury drops, will be published later [23].

In the extreme hypothetical case in which field (E)-induced polarization results in the surface charge (Q) concentrating at a point, the electrostatic force (EQ) would act against a viscous drag force, which for bubbles with a mobile interface at $Re < 1$, is $2\pi d\eta v$ [20]. Then the electrophoretic velocity would be given by

$$v = qEd/3\eta \qquad (3)$$

where q is the initially uniform charge density on the bubble of diameter d in a solution of viscosity η, so that the electrophoretic mobility ($u = v/E$) would vary linearly with bubble diameter, as observed experimentally (Fig. 12).

Fig. 13 shows a non-linear dependence of bubble electrophoretic mobility on electric field strength, which was attributed to polarization of the bubble surface charge density distribution. This interpretation is in contrast to the hydrodynamic argument offered in the case of a spinning electrophoresis cell [8]. Extrapolation of the curve in Fig. 13 to zero field strength gives an expected electrophoretic mobility of 3.5×10^{-8} m^2 s^{-1} V^{-1}, which represents the contribution made by bubble rise-induced hydrodynamic effects to the charge density distribution, and is the dominant effect for field strengths < 18 kV m^{-1}.

Fig. 14 shows the effect of electrolyte concentration on the electrophoretic mobility of

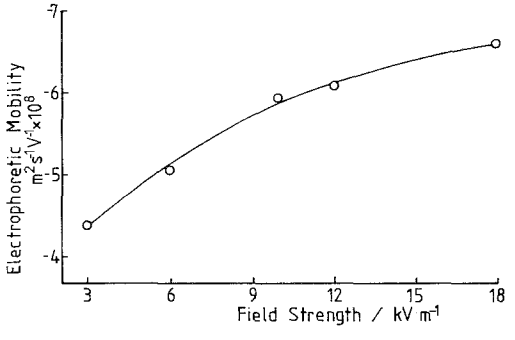

Fig. 13. Effect of electric field strength on the electrophoretic mobility of 100 μm hydrogen bubbles in 1 mol Na_2SO_4 m^{-3} at pH 6.8.

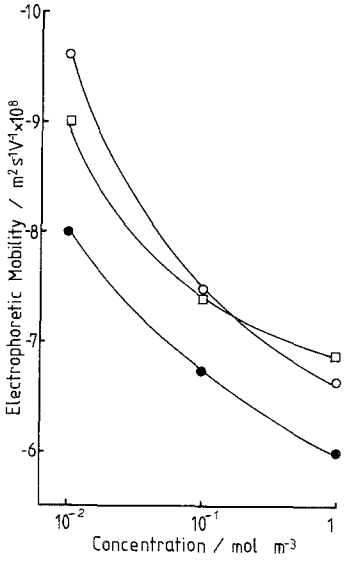

Fig. 14. Influence of electrolyte concentration on the electrophoretic mobility of 100 μm hydrogen bubbles at pH 6.9. • Na_2SO_4, □ $NaClO_4$, ○ $NaNO_3$.

bubbles in both 1 : 1 and 2 : 1 electrolytes. Electrophoretic mobilities decreased with electrolyte concentration [c] due to a reduced diffuse layer thickness, the charge density being assumed to remain constant [22]. Electrophoretic mobilities were greater in a 1 : 1 electrolyte, in which a more extensive diffuse layer is obtained [22].

To confirm that results were not being influenced by the experimental design, glass spheres of known diameter (40–120 μm) were deflected by the electric field as they fell between the electrodes. Their electrophoretic mobilities showed no diameter dependence, as expected for solid particles. The glass spheres were then crushed and their electrophoretic mobilities measured by conventional microelectrophoresis [22]. Good agreement was obtained between the two techniques, and with values reported in the literature, so validating the experimental procedure for bubbles.

3.3.2. Surfactant-containing electrolytes. Experiments were carried out to reverse the charge on a bubble in a solution at a given pH, by the addition of an oppositely charged surfactant. Interpolation of the results allowed the concentration of surfactant required to give zero electrophoretic mobility, and by inference zero charge, to be determined.

Figs. 15 and 16 describe the results obtained

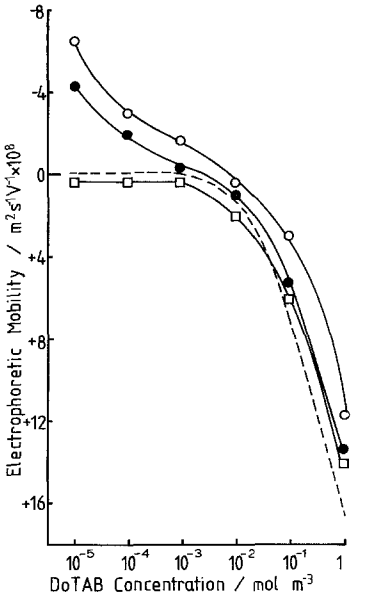

Fig. 15. Effect of DoTAB surfactant concentration on the electrophoretic mobility of 100 μm hydrogen bubbles in 1 mol $NaNO_3$ m^{-3} at pH 10.5 (○), 6.9 (●) and 2.4 (□). ——— electrophoretic mobility calculated from Gouy–Chapman Smoluchowski Equation 5, using independent adsorption isotherm data [19], and assuming a uniform charge density distribution.

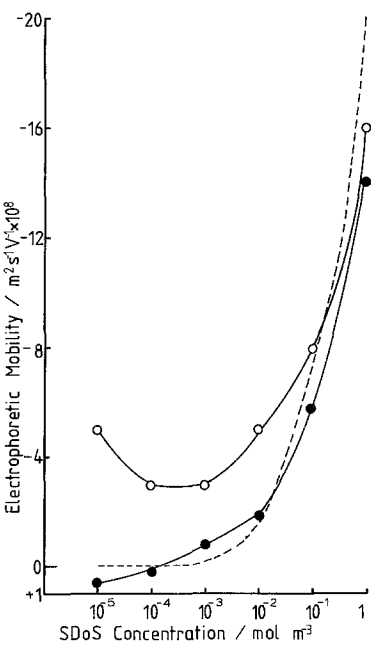

Fig. 16. Effect of SDoS surfactant concentration on the electrophoretic mobility of 100 μm hydrogen bubbles in 1 mol $NaNO_3$ m^{-3} at pH 2.4 (●) and 6.8 (○). ——— calculated as for Fig. 15.

with a cationic (DoTAB) and anionic (SDoS) surfactant in millimolar sodium nitrate. Fig. 15 shows that DoTAB concentrations of 4×10^{-3} and 8×10^{-3} mol m^{-3} were required to neutralize the initial charge on the bubble at pH 6.9 and 10.5, respectively. Extrapolation of the adsorption isotherm for DoTAB at the water–vapour interface [19] gave corresponding surface concentrations (Γ) of:

$$\Gamma(6.9) = 4.8 \times 10^{-9} \text{ mol m}^{-2}$$

$$\Gamma(10.5) = 9.6 \times 10^{-9} \text{ mol m}^{-2}$$

though it should be noted that Γ will be slightly higher in a millimolar electrolyte than in water. The bubble surface charge density can then be calculated at pH 6.9 and 10.5 as:

$$q(6.9) = -0.46 \text{ mC m}^{-2}$$

$$q(10.5) = -0.93 \text{ mC m}^{-2}$$

The bubble charge at pH 2.4 was obtained using the same procedure, but required an anionic surfactant (SDoS) to reverse the charge. Fig. 16 shows that a bulk concentration of 2×10^{-4} mol m^{-3}, corresponding to a surface concentration of 2.8×10^{-10} mol m^{-2}, was required to bring the bubble electrophoretic mobility to zero at pH 2.4. The surface charge density was then:

$$q(2.4) = +27 \,\mu\text{C m}^{-2}$$

Fig. 17 summarizes the influence of solution pH on both the charge density (q) of a stationary, unpolarized gas–liquid interface and the corresponding zeta potentials ζ calculated from [22]:

$$q = (4n_0 ze/k)\sin h(zF\zeta/2RT) \qquad (4)$$

If the Smoluchowski equation:

$$u = \epsilon\zeta/\eta \qquad (5)$$

were to be applied to the calculated zeta potentials, then it would predict electrophoretic mobilities of only $+0.03$ to -1.0×10^{-8} m^2 s^{-1} V^{-1} in a clean system. These are much lower than the value of $+1$ to -10×10^{-8} m^2 s^{-1} V^{-1} observed over the same pH range (Figs. 9–11). This illustrates that theories derived for solid particles cannot be applied to gas bubbles.

Figs. 15 and 16 also illustrate the influence of the rigidifying effect of surfactant adsorption at the bubble interface, on the bubble electroph-

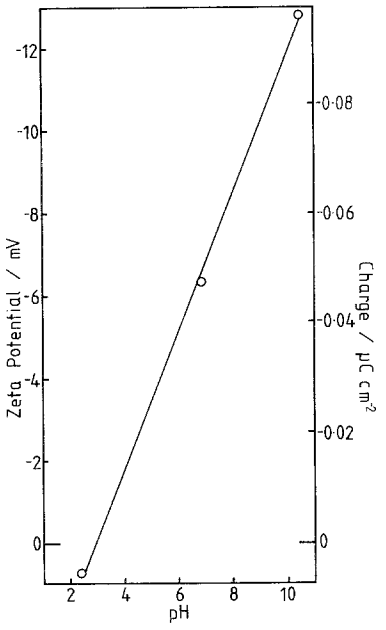

Fig. 17. The pH dependence of the calculated (Equation 4) zeta potential ζ and charge density (q) of the gas–aqueous solution interface.

oretic mobility. Low surfactant concentrations reduced the bubble electrophoretic mobility, even when bubble and surfactant were of like charge. Increasing the surfactant concentration further then raised the electrophoretic mobility, which tended towards that calculated for an equivalent solid particle of zero initial charge.

The decrease in mobility observed in Fig. 16 as the SDoS concentration increased from 10^{-5} to 10^{-4} mol m^{-3} arose from partial surface rigidifying, leading to reduced mobility of charge on the bubble surface and hence reduced electrophoretic mobility. The enhanced mobility and hence lack of full rigidification, persisted up to 10^{-2} to 10^{-1} mol SDoS m^{-3}, above which concentration, monolayer coverage was achieved.

Addition of millimolar sodium tetradecylsulphate, giving complete coverage of the bubble by surfactant, resulted in an electrophoretic mobility of 13.6×10^{-8} m^{-2} s^{-1} V^{-1} being measured at pH 6.8. This is a reasonable value for an immobile, non-polarized surface taking account of expected counter-ion absorption. Under these conditions bubble electrophoretic mobility was independent of the electric field strength, in contrast to the non-linear dependence observed in a clean system (Fig. 13). This is further evidence for the immobility of the gas–liquid interface with monolayer surfactant adsorption.

Acknowledgement

The authors thank the Science and Engineering Research Council (SERC) and Unilever Research plc for the provision of a CASE research studentship for NPB.

References

[1] H. A. McTaggart, *Phil. Mag.* **44** (1914) 297.
[2] *Idem, ibid.* **105** (1922) 386.
[3] T. Alty, *Proc. R. Soc.* **106** (1924) 315.
[4] *Idem, ibid.* **112** (1926) 235.
[5] C. Cichos, *Neue Bergbautechnik* **1** (1971) 941.
[6] *Idem, ibid.* **2** (1972) 928.
[7] R. W. Huddleston and A. L. Smith, in 'Foams', (edited by A. J. Akers) Academic Press, London (1976) pp. 147–160.
[8] J. A. McShea and I. C. Callaghan, *Colloid Polym. Sci.* **261** (1983) 757.
[9] S. Usui and H. Sasaki, *J. Colloid Interface Sci.* **65** (1978) 36.
[10] S. Usui, H. Sasaki and H. Matsukawa, *ibid.* **81** (1981) 80.
[11] T. Sotskova, Yu. F. Bozhenov and L. Kulskii, *Koll. Zh.* **44** (1982) 989.
[12] G. L. Collins and G. J. Jameson, *Chem. Eng. Sci.* **32** (1977) 239.
[13] G. L. Collins, M. Matarjemi and G. J. Jameson, *J. Colloid Interface. Sci.* **63** (1978) 69.
[14] Y. Fukui and S. Yuu, *AIChEJ.* **28** (1982) 866.
[15] J. C. Scott, in 'Symposium on Surface Contamination', Vol. 1 (edited by K. L. Mittal) Plenum, New York (1978) pp. 477–497.
[16] N. P. Brandon and G. H. Kelsall, *J. Appl. Electrochem.* **15** (1985) 475.
[17] N. P. Brandon, PhD Thesis, London University (1985).
[18] B. E. Conway, H. Angerstein-Kozlowska and W. B. A. Sharp, *Anal. Chem.* **45** (1973) 1331.
[19] B. McGhee, PhD Thesis, Manchester University (1966).
[20] V. G. Levich, 'Physicochemical Hydrodynamics', Prentice-Hall, New Jersey (1962) pp. 395–471.
[21] D. W. Moore, *J. Fluid Mech.* **16** (1963) 161.
[22] R. J. Hunter, 'Zeta Potentials in Colloid Science'. Academic Press, New York (1981).
[23] N. P. Brandon, G. H. Kelsall, S. Levine and A. L. Smith, to be published.